Synthesis of Binary Ti-Si Mixed Oxides Nanoparticles with Rutile Structure as Selective Catalyst for Epoxidation of Alkenes

Z. Fakhroueian,[1] F. Farzaneh,[1,*] and M. Ghandi[2]

[1]*Department of Chemistry, Alzahra University, Vanak, Tehran, Islamic Republic of Iran*
[2]*School of Chemistry, University College of Science, University of Tehran, Tehran, Islamic Republic of Iran*

Abstract

The nanoparticles of Ti-Si mixed oxides (NTSO) with Rutile structure were prepared by sol-gel method in a mixture of alcohol and water as solvent. The solid product was characterized by XRD, FTIR, SEM, TEM, UV, TGA and laser Raman spectroscopy. The catalytic activity of NTSO (5-10 nm) was investigated in the epoxidation of cis stilbene, trans stilbene, and norbornene by using oxidants such as tert-butylhydroperoxide (TBHP), molecular oxygen (O_2)/isobutyraldehyde (IBA) and hydrogen peroxide (H_2O_2). It was found that epoxides of trans-stilbene and norbornene were formed quantitatively with the green H_2O_2 oxidant during 12 h.

Keywords: Epoxidation; Alkenes; Ti-Si mixed oxides; Nanoparticles; Heterogeneous catalysis

1. Introduction

Direct epoxidation of olefins on Ti-containing porous dioxide such as zeolites, mixed oxides and mesoporous materials (MCM'S) has received considerable attention during the last few years. Ti-substituted silicalite-1(TS-1) was found to be a good catalyst for epoxidation of small size olefins with H_2O_2. It was also found that a variety of Ti-zeolites such as TS-2, Ti-ITQ, Ti-ZSM-12 were active catalysts for epoxidation of olefins [1-5]. The special activity of TS-1 was assigned to the tetrahedrally coordinated Ti in the framework, its hydrophobic nature, and Lewis acidic Ti (IV) sites. Ti-MCM-type materials are another group of catalysts for double bond epoxidation. By grafting Ti-complex to Ti-MCM-41, the higher activity and selectivity was obtained.

The TiO_2-SiO_2 mixed oxides have been reported to have higher catalytic activity and selectivity with respect to pure TiO_2 [6-9]. TiO_2 and SiO_2 mixed oxides have been used as catalysts for a number of different reactions such as phenol amination [10], butene isomerization [11], cumene dealkylation [8,12], and olefin epoxidation [13]. Recently, nanocatalysts have attracted much attention due to their higher activity and selectivity which have been attributed to their large specific surface area, high percentage of surface atoms and special crystal structures [14].

In this study, synthesis of NTSO and their catalytic activities for epoxidation of olefins with different oxidants will be discussed.

2. Experimental

2.1. Materials

TBHP (80% in di-tert-butyl ether), acetonitrile, H_2O_2

---

* Corresponding author, Tel.: +98(21)88258977, Fax: +98(21)66495291, E-mail: faezeh_farzaneh@yahoo.com

Table 1. Results of catalytic epoxidation of some olefins with TBHP in the presence of NTSO

Olefin	Time (h)	Total Conversion (%)	Epoxy (%)	Others (%)	TON[a]
Trans-stilbene	9	86	100	–	54
	12	100	100		63
Cis-stilbene	9	45	100	–	57
	12	73	100		92
Norbornene	9	55	100	–	688
	12	100	100		1250

Reaction conditions: trans-stilbene, cis-stilbene, norbornene, 1 mmol, 2 mmol, 20 mmol, respectively.

[a]TON: mmol product/mmol catalyst.

(35%), methanol, tetraethylorthosilicate (TEOS) (99%), titanium (IV) isopropoxide (TIPO) (97%), 2-propanol, cis and trans-stilbene, norbornene and IBA were purchased from Merck Chemical Company, and used without further purification.

2.2. Instrumentation

Powder X-ray diffraction (XRD) data were recorded on XRD 3003 PTS Seifert with Cu Kα radiation (λ=1.54Å). FTIR spectra were measured on KBr disks with a Bruker-Tensor 27 2002 spectrometer. Scanning electron micrograph (SEM) images were taken by XL-30 Phillips (1992). High resolution transmission electron microscopy (HRTEM) was performed by using TECNAI F20 field emission gun microscope operating at 200 KeV and equipped with Gatan 794 slow scan charge-coupled device camera. Nitrogen adsorption and desorption isotherm was carried out on an ASAP 2000 micrometrics gas sorption analyzer. Surface areas were calculated by the Brunauer-Emmett-Teller (BET) method by N_2 gas with Quanta chrome chembet 3000. The pore size was calculated using the Barrett-Joyner-Hatenda (BJH) model. The bond-gap energy was measured to be 2.91 eV by Epps 2000 stellar Net Inc photo spectrometer. TGA thermal curve was studied by Perkin-Elmer Pyrif 1. The oxidation products were analyzed by GC and GC-Mass using Agilent 6890 series, with FID detector and HP-5ms 6890 Network GC system respectively. The Raman spectrum was record by using the Almega Dispersive Raman Spectrometer Thermo-NICOLET 2003 American.

2.3. Preparation NTSO

The reported procedure for the synthesis of Ti-Si mixed oxides was adopted and partially modified as follows [15]. TEOS (15 g) in 2-propanol (50 ml) was slowly added to TIPO (20 g) in 2-propanol (50 ml).

After stirring for several minutes, deionized water (11 ml) was injected during 3-4 h by a syringe pump. The solid product was then separated, dried and calcined at 850°C for 8 h.

2.4. Oxidation of Alkenes with THBP or H_2O_2: General Procedure

A mixture of catalyst (0.24 g) and appropriate amount of alkene (see Table 1) was stirred in CH_3CN (8 ml) under nitrogen atmosphere. TBHP (24 mmol), or H_2O_2 (1.2 ml, 30%) was then added and the mixture was refluxed for 9 and 12 h. After filtration, the solid was washed with solvent and the filtrate was then subjected to GC and GC-Mass analysis.

2.5. Oxidation of Alkenes with O_2 / IBA: General Procedure

To a mixture of catalyst (0.24 g) and alkene (20 mmol in 8 ml CH_3CN) was added IBA (24 mmol). The mixture was refluxed under O_2 atmosphere for 12 h. It was then filtered, washed with fresh CH_3CN and the filtrate was subjected to GC and GC-Mass analysis.

3. Results and Discussion

3.1. Characterization of Catalyst

Figure 1 shows the X-ray powder diffraction pattern of calcined NTSO at 850°C which is exactly consistent with Rutile structure [15,16].

The nitrogen adsorption-desorption isotherm plots of calcined NTSO is shown in Figure 2. The isotherms indicate that at low relative pressures P/P_o, adsorption takes place as a thin layer on the walls (monolayer of coverage). Sharp inflection point at $P/P_o = 0.93$ was found. The BET specific surface area of NTSO is 46 m^2/g. The pore size distributions was measured by

Barrett-Joyner-Hatenda (BJH) model [9,17,18],and mercury techniques. It can be observed that the pore sizes of the sample concentrate in a range of 5-10 nm and mean pore size is 7 nm and the total pore volume is 0.1 cm^3/g and wall thickness is 0.5 nm.

The UV-Vis spectrum of the calcined NTSO is shown in Figure 3. As seen, one broad intense band appears at 440 nm is characteristic of titanium atoms in a tetrahedral coordination sphere [15].

The FTIR spectrum of NTSO is shown in Figure 4. Two bands appear at 466 and 1087 cm^{-1} are assigned to the Si-O-Si bending mode and asymmetric stretching vibration respectively. The band at 948 cm^{-1} represents the Ti-O-Si linkage. The peaks observed at 1623 and 3234 cm^{-1} are assigned to the stretching vibrations of OH group and molecular H_2O [9,15,18].

Figure 5 shows the TGA curve of NTSO. A weight loss at around 100°C, is due to desorption of physically bonded water and surface dehydroxylation. By increasing the temperature, the TGA curve becomes smooth and the weight lose is completely constant at around 600°C. The results indicate that water and organic residues in the mixed oxide were completely removed above 200°C [19].

Transmission electron microscopy (TEM) image of calcined NTSO is shown in Figure 6. The lattice fringe of ~0.35 nm was observed, which corresponds to the lattice spacing of a plane in the Rutile phase [20].

Laser Raman spectrum of NTSO is shown in Figure 7. It exhibits two sharp peaks at 650 and 750 cm^{-1} and a broad peak at 430 cm^{-1}, which are consistent with Rutile spectrum of TiO_2. The position of peaks shifts to higher wave numbers due to the silicon incorporation into the sample [15].

3.2. Catalytic Activity

3.2.1. NTSO as Catalyst for Epoxidation of Trans-stilbene, Cis-stilbene and Norbornene with TBHP Oxidant

Results obtained in the epoxidation of trans-stilbene, cis-stilbene, and norbornene with TBHP as oxidant in the presence of NTSO catalyst are shown in Table 1. As seen in Table 1, trans-stilbene and norbornene quantitatively and cis-stilbene about 73% are converted to the corresponding epoxides during 12 h. Such observation is not surprising on the basis of the reaction mechanism (*vide infra*). The formation of epoxide with 100% selectivity in these cases is remarkable.
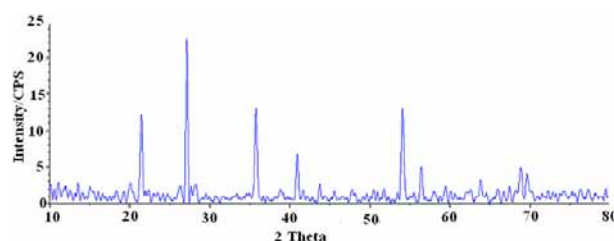

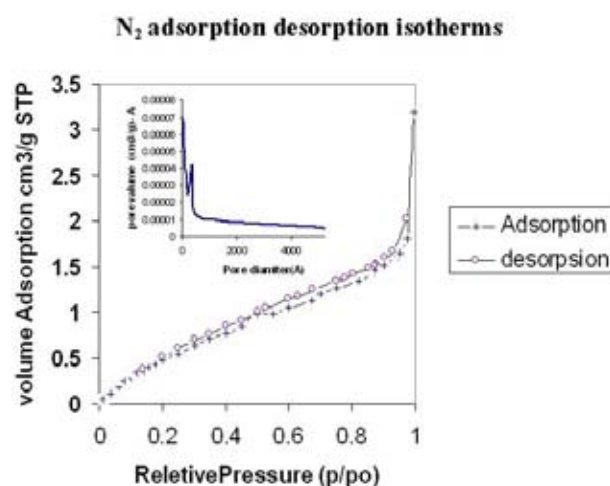**Figure 1.** XRD pattern of NTSO with Rutile structure.

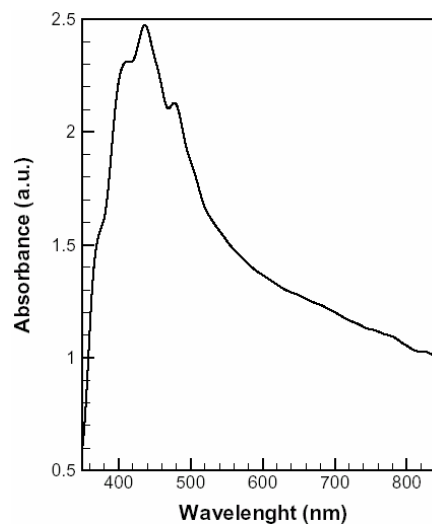**Figure 2.** Nitrogen adsorption isotherms and pore size distribution of NTSO.

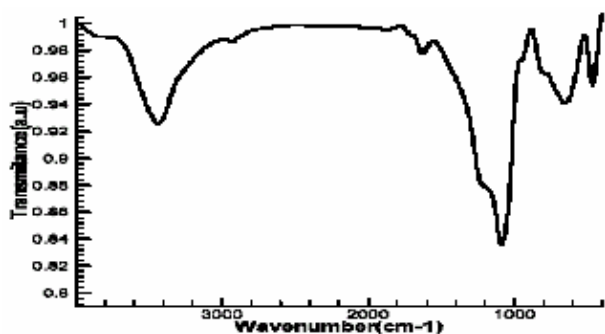**Figure 3.** UV-Vis absorption spectrum of NTSO.
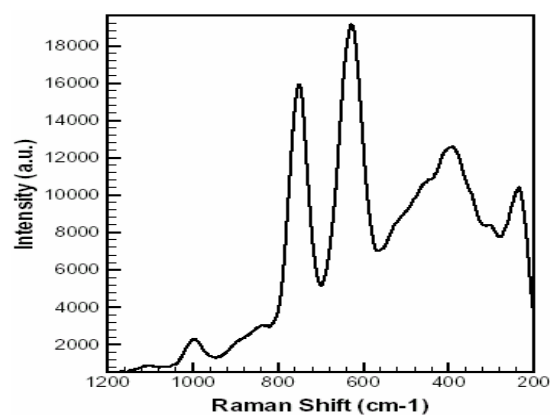
Figure 4. FT-IR of TiO_2-SiO_2 calcined at 850°C.

Figure 7. Laser Raman spectrum of NTSO.

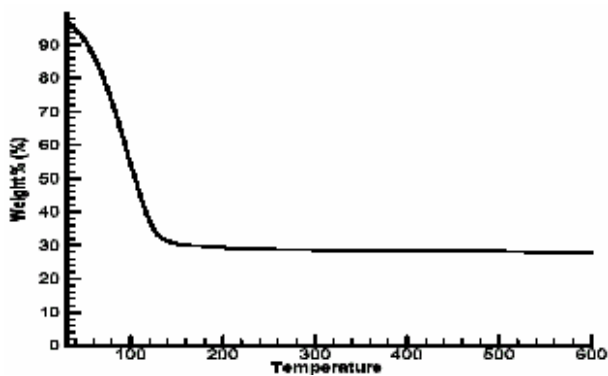**Figure 5.** TGA curve of Ti-Si mixed oxides up to 850°C.

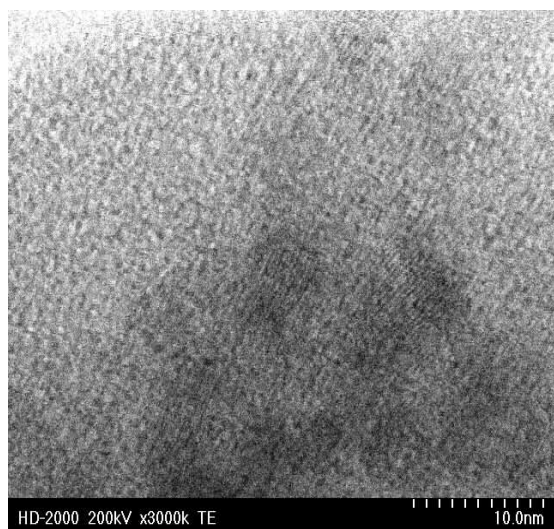**Figure 6.** TEM image of nanosized TiO_2/SiO_2 (1:1).

3.2.2. NTSO as Catalyst for Epoxidation of Trans-stilbene and Norbornene with O_2/IBA and H_2O_2

As seen in Table 2, utilization of oxygen with isobutyraldehyde in acetonitrile as solvent, will lead to 100% conversion of trans-stilbene and norbornene with 70-79% selectivity toward the corresponding epoxides. Surprisingly, trans-stilbene and norbornene have quantitatively been converted to the corresponding epoxides by using H_2O_2 as oxidant (see Table 2). Since H_2O_2 is a green oxidant, the formation of the epoxides in 100% yields is promising.

It was found that 2-cyclohexene-1-one and cyclohex-2-enyl-1-tert-butyl peroxide (mixed peroxide) were formed as the major products in the oxidation of cyclohexene with TBHP in the presence of NTSO catalyst. Based on the work of Sherington and his co-workers, the formation of the mixed peroxide is a strong evidence of t-BuOO radical implication in oxidation reaction [21]. Our previous experience is in agreement with Sherington's viewpoint since the operation of a radical pathway mechanism in cyclohexene oxidation with TBHP catalyzed by immobilized Vitamin B_{12} within MCM-41 affording 2-cyclohene-1-one and cyclohex-2-enyl-1-tert-butyl peroxide products was supported by observing the total quenching of the products in the presence of Ph_2NH radical scavenger [22]. Therefore, it is plausible that the free radical species which are responsible for alkene oxidation are formed via outer-sphere electron transfer from TBHP to catalyst in a Haber-Weiss type mechanism. Since cyclohexene contains active allylic hydrogens, the t-BuOO radical is scavenged by abstracting a hydrogen atom leaving the stable cyclohexene radical. Subsequent reaction of this intermediate with TBHP will finally

Table 2. The results of epoxidation of trans-stilbene and norbornene with different oxidants

Substrate	Oxidant	Conversion (%)	Product (%)		TON
			Epoxide	*Other*	
Trans-Stilbene	TBHP	100	100	–	63
	O₂/IBA	100	70	30[a]	63
	H₂O₂	100	100	–	63
Norbornene	TBHP	100	100	–	1000
	O₂/IBA	100	79	21[a]	1000
	H₂O₂	100	100	–	1000

Reaction conditions: trans-stilbene, 1 mmol, norbornene, 20 mmol, time, 12 hours; TON: mmol products/mmol catalyst.
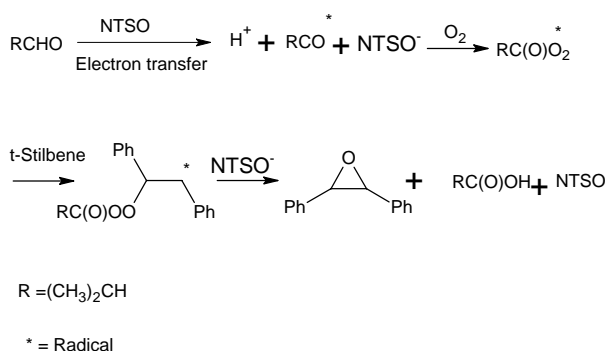[a]Unidentified product(s).
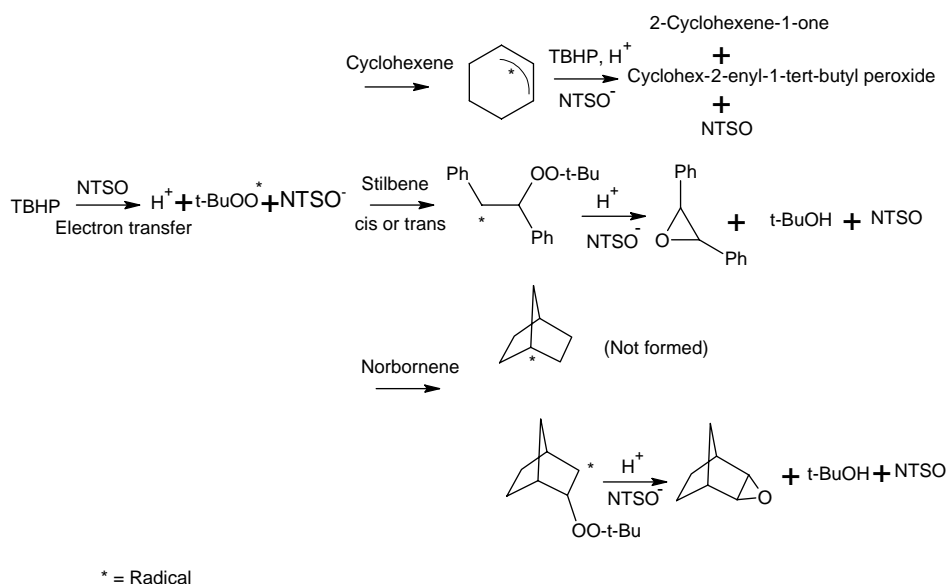
Scheme 1

yield the oxidation products (Scheme 1). On the other hand, since cis and trans-stilbenes do not contain allylic hydrogens in their molecular structures, addition of peroxy radical to double bond with subsequent epoxide formation is inevitable (Scheme 1). That norbornene containing allylic hydrogens in the molecular structure affords the corresponding epoxide is easily inferred by knowing the fact that the formation of the unstable bridgehead radical is not possible under the reaction conditions (Scheme 1) [23].
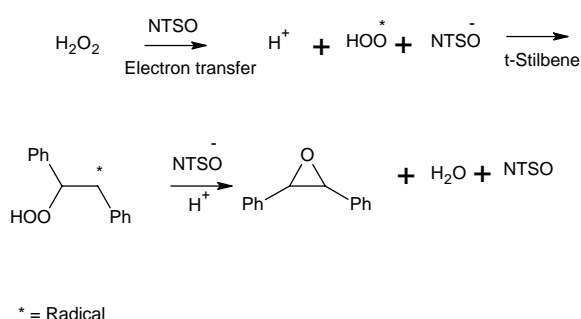
It seems likely to believe that isobutylperoxy radical as the key oxidant has probably been produced via outer-sphere electron transfer from aldehyde to NTSO (Scheme 2) [24]. Addition of this radical to trans-stilbene with subsequent degradation affords the corresponding epoxide.

To make insight into the oxidation reaction mechanism with H₂O₂, we used the oxygen-radical trap Ph₂NH. Using an equimolar of trapping agent with H₂O₂ completely suppressed either trans-stilbene or norbornene oxidations based on the GC analysis of the products mixture, which showed that the alkenes were left intact. Therefore, similar mechanism to that of TBHP oxidation is anticipated (Scheme 3).

$$RCHO \xrightarrow[\text{Electron transfer}]{NTSO} H^+ + RCO^* + NTSO^- \xrightarrow{O_2} RC(O)O_2^*$$

t-Stilbene

$$\xrightarrow{} \underset{RC(O)OO}{\overset{Ph}{\underset{}{C^*}}}\overset{Ph}{\underset{}{} } \xrightarrow{NTSO^-} \underset{Ph}{\overset{O}{\triangle}}\underset{Ph}{} + RC(O)OH + NTSO$$

$R = (CH_3)_2CH$

* = Radical

Scheme 2

$$H_2O_2 \xrightarrow[\text{Electron transfer}]{NTSO} H^+ + HOO^* + NTSO^- \xrightarrow{\text{t-Stilbene}}$$

$$\underset{HOO}{\overset{Ph}{\underset{}{C^*}}}\underset{Ph}{\overset{}{}} \xrightarrow[H^+]{NTSO^-} \underset{Ph}{\overset{O}{\triangle}}\underset{Ph}{} + H_2O + NTSO$$
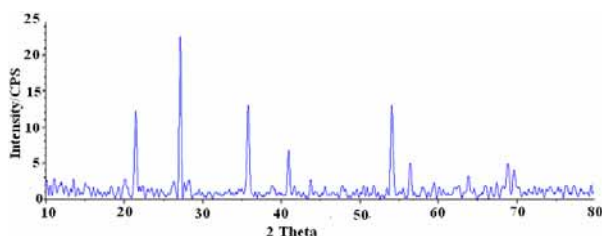
* = Radical

Scheme 3

Figure 8. X-ray diffraction pattern of NTSO after using as catalyst for four times.

Although catalytic activity of $Ti(IV)/SiO_2$ has been reported to be superior due to an increase in Lewis acidity, it is ineffective catalyst for epoxidation with aqueous hydrogen peroxide [24]. This effect arises by the strongly coordinating ligands, especially water [24]. On the contrary, our NTSO catalysis system is remarkably active with aqueous H_2O_2 (see Table 2). The remarkable activity of NTSO in epoxidation with

aqueous H_2O_2 is attributed to site-isolation of Ti centers in the hydrophobic pores of silicates which allows for the simultaneous adsorption of the oxidant and the hydrophobic alkene in the presence of water [24]. The difference between $Ti(IV)/SiO_2$ and NTSO might arise either from crystallinity of the latter in comparison to the former or the very higher calcination temperature of 850°C which we used in NTSO synthesis.

Therefore, approach of H_2O_2 to Ti in the absence of deactivating water molecules present in the vicinity of reaction center produces the peroxy radical via one-electron transfer process. Subsequent addition to alkene double bond and elimination of water affords the corresponding epoxide (Scheme 3).

3.3. Characterization and Identification of Catalyst after Recycling of NTSO

In order to evaluate the activity of the recycled NTSO, the epoxidation reactions were carried out for four times. The catalyst was recalcined before each step in order to eliminate the adsorbed products. It was found that the catalytic activity remained almost constant after fourth runs and the products yields were similar. Moreover, no Ti was detected in solution. Particularly significant is the fact that no structural changes occurred in the catalyst (NTSO) throughout the cycles based on the XRD pattern (Fig. 8). Therefore, it can be concluded that the nanoparticles of NTSO exhibit good stability under the reaction conditions. It was regenerated repeatedly without losing activity.

Conclusion

In this work, we have prepared the nanoparticles of NTSO with Rutile structure in a mixture of alcohol and water. It shows excellent catalytic activity and selectivity for epoxidation of trans-stilbene and norbornene with TBHP, O_2/IBUA and eco-friendly H_2O_2 oxidants.

Acknowledment

References

1. Sheldon R.A. *J. Mol. Catal. A: Chem.*, **107**: 75 (1996).
2. Taramasso M., Perego G., and Notari B. *US Patent*, **4**: 410-501 (1983).
3. Notari Stud B. *Surf. Sci-Catal.*, **37**: 413 (1983).
4. Muller C.A., Maciejewski M., Mallat T., and Baiker A. *J.*

Catal., **184**: 280 (1999).

5. Deng Y. and Maier W.F. *Ibid.*, **199**: 115 (2001).

6. Corma A. *Top. Catal.*, **4**: 249 (1997).

7. Davies L.S., Mc. Morn P., Bethell D., Bulman Page P.C., King F., Hancock F.E., and Hutchings G.J. *J. Catal.*, **198**: 319 (2001).

8. Cagnoli M.V., Casuscelli S.G., Alvarez A.M., Bengoa J.F., Gallegos N.G., Samaniego N.M., Crivello M.E., Ghione G.E., Perez C.F., Herreo E.R., and Marchetti S.G. *Appl. Catal. A: Gen.*, **287**: 227 (2005).

9. Eimer G.A., Casucelli S.G., Ghione G.E., Crivello M.E., and Herrero E.R. *Ibid.*, **298**: 232 (2006).

10. Itoh M., Hattori H K., and Tanabe K. *J. Mol. Catal.*, **35**: 225 (1974).

11. Nakabayahi H. *Bull. Chem. Soc. Japn.*, **65**: 914 (1992).

12. Hutter R., Mallat T., and Baiker A. *J. Catal.*, **153**: 177 (1995).

13. Sohn J.R., and Jang H.J. *Ibid.*, **132**: 563 (1991).

14. Martinez-Mendez S., Heriquez Y., Dominguez O., D'ornelas L., and Krentzien K. *J. Mol. Catal. A: Chem.*, **252**: 226 (2006).

15. Liu Z., and Davis R.J. *J. Phys. Chem.*, **98**: 1253 (1994).

16. Zhang X., Zhang F., and Yu Chan K. *Appl. Catal. A: Gen.*, **284**: 193 (2005).

17. Lynch J. *Physico-Chemical Analysis of Industrial Catalysts*. Edition Technip, Paris, 6-22 (2003)

18. Beck C., Mallat T., Burgi T., and Baiker A. *J. Catal.*, **204**: 428 (2001).

19. Xie C., Xu Z., Yang Q., and Xue B.J. *Du Zhang J, Mater. Sci. and Eng. B*, **112**: 34 (2004).

20. Kwon C.H., Kim J.H., Jung I.S., Shin H., and Yoon K.H. *Ceramics International*, **29**: 851 (2003).

21. Olason G. and Sherrington D.C. *Reactive & Functional Polymers,* **42**: 163 (1999).

22. Farzaneh F., Taghavi J., Malakooti R., and Ghandi M. *J. Mol. Catal. A: Chem.*, **244**: 252 (2006).

23. March J. *Advanced Organic Chemistry*. Third Edition, John Wiley & Sons, New York, p. 616 (1985).

24. Arends J.W.C.E. and Sheldon R.A. *App. Catal A: Gen.*, **212**: 175 (2001).